Characterization of Eroded Boron Atoms in the Plume of a Hall Thruster

IEPC-2013-158

Presented at the 33rd International Electric Propulsion Conference,
The George Washington University, Washington, D.C., USA
October 6–10, 2013

Horatiu C. Dragnea* and Iain D. Boyd†
University of Michigan, Ann Arbor, MI, 48109, U.S.A.
Brian C. Lee‡ and Azer P. Yalin§
Colorado State University, Fort Collins, CO, 80523, U.S.A.

Abstract: The erosion of boron particles from Hall thruster channel walls is a concern because it limits the lifetime of the device. A new optical experimental technique that measures path integrated boron number density in the plume of a Hall effect thruster has recently been tested on a SPT-70 thruster. The data obtained may be used to infer the channel wall erosion rate, but further knowledge of the flow field is required. This development and the need to obtain a complete picture of the thruster channel and plume flows prompted a numerical simulation of the thruster erosion process. The direct simulation Monte Carlo method is used to study the sputtered boron atoms. These particles are introduced to the computational domain with velocities consistent with the sputtering process. The number flux is derived from a Sigmund-Thompson velocity distribution function. The number density values obtained in the plume are processed and compared to the measured values. The experimental and simulation results agree qualitatively, and disagree quantitatively by a factor of $3-4$, with the experimental results having lower values. Various causes of the discrepancy are discussed.

Nomenclature

Γ	= particle flux
f_n	= distribution function for normal velocity component
f_t	= distribution function for tangential velocity component
g	= generic function
k_B	= Boltzmann constant
m_B	= mass of boron
m_N	= mass of nitrogen
n	= number density
R	= radial coordinate
v_n	= normal velocity component
v_t	= tangential velocity component
Z	= axial coordinate

*Graduate Student Research Assistant, Aerospace Engineering, horatiud@umich.edu.
†James E. Knott Professor, Aerospace Engineering, iainboyd@umich.edu.
‡Graduate Student Research Assistant, Physics, blee66@rams.colostate.edu
§Associate Professor, Mechanical Engineering, ayalin@engr.colostate.edu

I. Introduction

HISTORICALLY, the main failure mode of Hall thrusters has been the erosion of its insulating channel walls. Moreover the eroded material from the plume may deposit on sensitive spacecraft surfaces such as solar panels, thus limiting the expected mission duration. Hence, added knowledge of the erosion process can provide valuable information about the thruster lifespan and a better understanding of the physical processes involved. Presently, the thruster lifetime is determined by operating the thruster in a vacuum chamber for a long duration, until significant damage to the walls is observed and quantified. Some methods for characterizing the damage, like multilayer chip erosion[1], involve modifying the channel walls to include several tracer materials that can be easily tracked during the erosion process. Yet this only provides localized information, and requires special machining of the thruster walls. Hence, of particular interest, is the development of a non-intrusive technique that can be used during testing, which does not require thruster wall alterations or extended thruster operation. This would provide significant cost benefits as well as reduced interference with the plasma. A cavity ring-down spectroscopy (CRDS) technique was developed by Lee *et. al.*[2] to satisfy these requirements. The procedure provides line integrated values of sputtered boron number density in the plume, measured at a distance of 2 mm away from the thruster exit plane. CRDS records the number of boron atoms in the ground electronic state. Thus atoms that are excited to higher states, or those becoming ionized are not accounted for. A computer simulation of a SPT-70 Hall effect thruster (HET) is developed and the results are compared to those measured experimentally in the plume.

The Procedure section describes how the boron sputtering process is modeled in the simulation (II.A), the numerical simulation set-up (II.B), and how the results are post-processed to obtain line-integrated number density values (II.C). The results are then presented and discussed in Section III. Conclusions and suggested future work are provided in Section IV.

II. Procedure

In the present case, only neutral boron and xenon atoms are being considered, and electromagnetic plasma effects are neglected. The computer code used for the simulation, MONACO[3], is an implementation of the direct simulation Monte Carlo method (DSMC)[4]. The program may be run on both scalar and parallel systems, and the results presented below are obtained after executing the code on 10 processors. A new type of boundary condition is developed specifically to simulate the erosion of boron atoms from the thruster walls. Boron atoms are introduced from the wall at a rate consistent with the erosion process, and the velocities of the boron atoms are assigned by sampling from the appropriate velocity distribution functions (VDFs). The wall does not recede in time, but due to the relatively short real-time duration of the simulation (0.015 seconds), this factor has minimal impact on the results. Two cases are considered: first the boron atoms simply reflect back into the domain upon colliding with a thruster wall surface, while in the second case the boron neutrals stick to the wall.

II.A. Modeling the Sputtering Process

The sputter boundary condition reproduces the physics of the wall sputtering process. The number of particles introduced through a given area, in a particular time interval, is derived from the sputtered boron particle flux, as explained in Section II.A.3. The velocities assigned to the new particles are sampled from the corresponding boron VDFs through acceptance-rejection sampling[4]. A brief description of the VDFs is provided in Section II.A.2.

The erosion boundary condition in MONACO requires an input value for the number density of material being eroded. By analyzing the geometry of the thruster, the volume of eroded material may be computed, and this is described in Section II.A.1. Considering the thruster operation time, an approximate value of the erosion rate will be computed. Although the real erosion rate is not constant, but decreases in time[5], the short real-time duration of the simulation ensures this approximation will not greatly influence the results. Finally, the required value for boron number density can be calculated by combining the volume flow rate with knowledge of the sputtered atoms' VDFs.

II.A.1. Volumetric Erosion Rate

The geometry of the SPT-70 used in Lee's CRDS experiment[2] was recorded by profilometer measurements. Linear functions that reproduce the profiles are illustrated in Fig. (1). It is assumed that before the thruster was first operated, both lines shown in Fig. (1) were horizontal. Thus to compute the volume eroded from the inner channel wall, the volume of rotation around the horizontal axis corresponding to the shape in Fig. (1a) is subtracted from the area of a circular cylinder of the same axial length and constant radius of 0.020 m. Similarly, the eroded volume from the outer channel wall is computed by subtracting the volume of rotation of the curve in Fig. (1b) from that of an annular circular cylinder of the same axial length and outer radius equal to the maximum hight of the profile, and constant inner radius of 0.035 m.

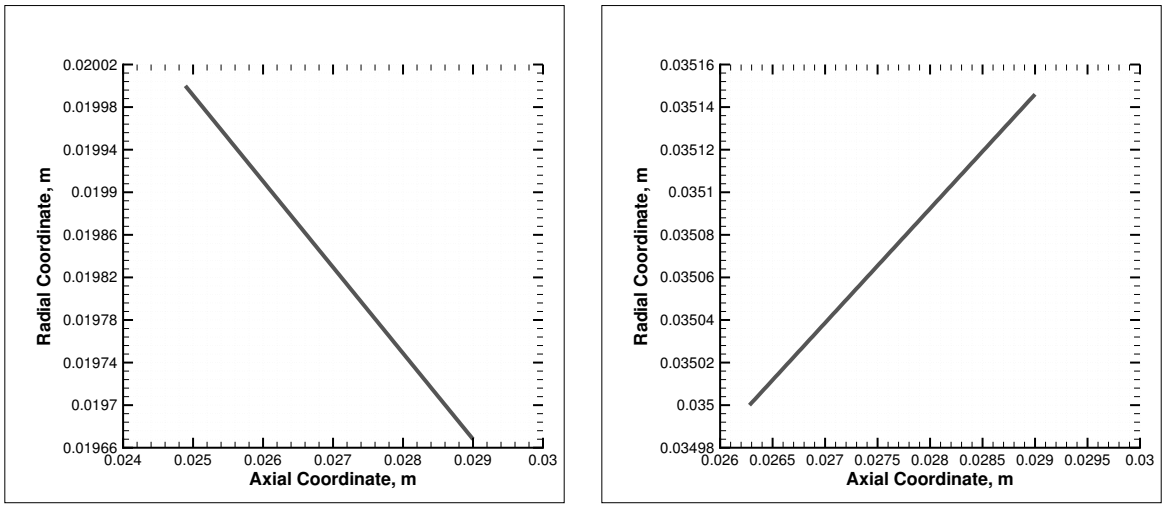

(a) Inner channel wall

(b) Outer channel wall

Figure 1: Measured erosion profiles for the SPT-70.

Following the procedure outlined above, the volume of eroded material from the outer channel wall is found to be $V_{outer} = 4.37 \times 10^{-8}$ m^3, and that from the inner channel wall, $V_{inner} = 8.53 \times 10^{-8}$ m^3. The total operation time for the HET is estimated to be 40 hours ($\pm$ 50% uncertainty), therefore the total volumetric erosion rate for the SPT-70 is:

$$\dot{V} = 8.96 \times 10^{-13} \text{ m}^3/\text{s} \tag{1}$$

II.A.2. Erosion VDFs

Smith and Boyd[6] have studied the sputtering of boron nitride due to xenon impact and obtained VDFs for boron atoms from a moleculat dynamics (MD) simulation at 100 eV energy and 45° angle of incidence. Similar functions were also found experimentally by Tao and Yalin[7], confirming the simulation results. In the direction perpendicular to the eroding wall, the VDF is of the Sigmund-Thompson form given in Eq. (2), and it is plotted in Fig. 2a. The VDF in the directions tangential to the wall is described by a bimodal Maxwellian in Eq. (4) and illustrated in Fig. (2b). Note that the same distribution function, f_t, is used for two directions, so the sampling is done twice in order to obtain independent results for each of the two velocity components that define the plane tangential to the wall.

$$f_n(v_n) \propto \frac{v_n^3}{(v_n^2 + v_b^2)^{3-2m}} \tag{2}$$

where the constants are defined as: $v_b = 5.25 \times 10^3$ m/s and $m = 0$.

$$f_t(v_t) \quad \propto \quad \sigma g_1(v_t) + (1-\sigma) g_2(v_t) \tag{3}$$

$$g_{1,2}(v_t) = \sqrt{\frac{m_B}{2\pi k_B T_{1,2}}} \cdot exp\left[-\frac{m_B(v_t - c_{1,2})^2}{2k_B T_{1,2}}\right] \tag{4}$$

where the constants are defined as: $\sigma = 0.552$, $c_1 = -1.75 \times 10^3$ m/s, $c_2 = -8.56 \times 10^3$ m/s, $T_1 = 2.62 \times 10^4$ K and $T_2 = 3.86 \times 10^4$ K.

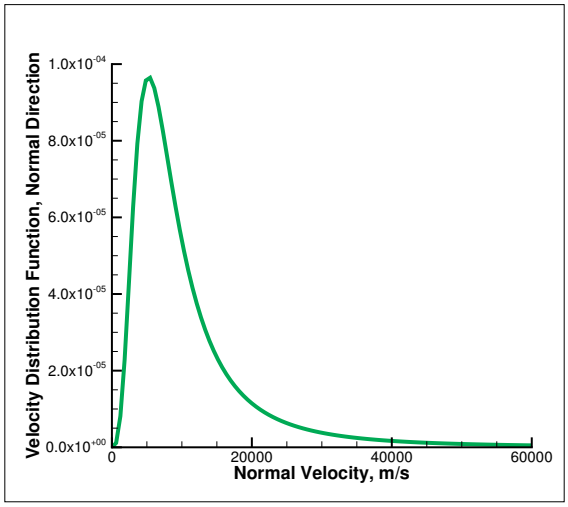

(a) Sigmund-Thompson

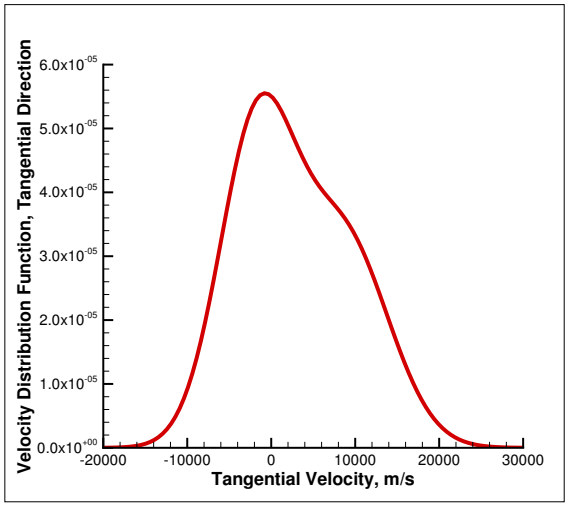

(b) Bimodal Maxwellian

Figure 2: Normalized velocity distibution functions for sputtered boron.

II.A.3. Computing the Boron Particle Flux

The number flux of particles that pass through a surface, in the direction perpendicular to it, may be expressed as:

$$\Gamma = \int_0^\infty n v_n f_{[n-\rho]}(v_n) dv_n \tag{5}$$

where $f_{[n-\rho]}$ is the density-based normalized VDF in the direction orthogonal to the wall surface. Introducing a normalization constant, $C_n = 7.39 \times 10^{11}\ m^3/s^3$, the distribution function is of the form:

$$f_{[n-\rho]}(v_n) = C_n \cdot \frac{v_n^2}{(v_n^2 + v_b^2)^{3-2m}} \tag{6}$$

where m and v_b are the same as in Eq. 2. Using Eq. 6, Eq. 5 is re-written as:

$$\Gamma = nC_n \int_0^\infty \frac{v_n^3}{(v_n^2 + v_b^2)^{3-2m}} dv_n \tag{7}$$

Since evaluating the integral in Eq. 7 in the limit at infinity does not yield meaningful results, it is evaluated at a finite upper bound. This value is chosen to be 6×10^4 m/s. It can be seen in Fig. (2a) that most of the VDF is included below this upper velocity bound. For simpler notation, the integral is renamed I:

$$I = C_n \int_0^{6\times10^4} \frac{v_n^3}{(v_n^2 + v_b^2)^{3-2m}} dv_n \tag{8}$$

The flux becomes:

$$\Gamma = nI \tag{9}$$

Numerical evaluation of Eq. 8 yields $I = 824.34$ m/s.

Note that the rate at which particles are introduced through a given surface area, A, is given by:

$$\dot{N} = A \cdot \Gamma \tag{10}$$

Thus, over a given surface area A, and in a time interval Δt, the number of particles introduced in the simulation, based on the value of the flux from Eq. 9, is:

$$\Delta t \cdot A \cdot \Gamma = \Delta t \cdot \dot{N} \tag{11}$$

Although the choice for an upper integration limit used in the numerical evaluation of Eq. 8 is arbitrary, the use of different values will not affect the simulation results. Using a higher value will increase I by a small increment, and the reverse will happen with the choice of a lower value. The factor I is used in the code to compute the particle flux, and the two variables are directly proportional. However, as shown in Section II.A.4, the input value of number density is inversely proportional to I. Therefore any changes in the computation of I will be implicitly accounted for.

II.A.4. Boron Number Density Values

Recall that the sputter boundary condition for the simulation requires a value for the boron number density. A reasonable value may be derived from the volumetric erosion rate that was computed in Section II.A.1. The first step is to calculate the mass flow rate of sputtered material, which is HBC grade boron nitride[5]. Its density is well known[8], and defined as $\rho_{HBC} = 1950$ kg/m^3. The procedure described below to compute the mass flow rate is applied to both the inner and outer channel walls, yielding values for the two number densities, respectively.

$$\dot{m}_{HBC} = \dot{V} \cdot \rho_{HBC} \tag{12}$$

Next, the mass flow rate may be expressed as:

$$\dot{m} = m_B \cdot \dot{N}_B + m_N \cdot \dot{N}_N \tag{13}$$

where $\dot{N}_B$ and $\dot{N}_N$ are particle erosion rates for boron and nitrogen, respectively. Assuming the value of these rates is the same for boron and nitrogen, the boron erosion rate may be denoted as $\dot{N}$ and computed as:

$$\dot{N} = \frac{\dot{m}}{m_B + m_N} \tag{14}$$

Combining Eqs. 9 and 10, the number density may be expressed as:

$$n = \frac{\dot{N}}{I \cdot A} \tag{15}$$

All the information on the right hand side of Eq. 15 is known, thus numerical values for the inner and outer channel walls are obtained:

$$n_{outer} = 1.32 \times 10^{16} \text{ m}^{-3} \tag{16}$$

$$n_{inner} = 4.40 \times 10^{16} \text{ m}^{-3} \tag{17}$$

Now consider the case where boron atoms consequently stick to the walls, upon colliding with any thruster surfaces. To account for the loss of particles due to the sticking process, the eroded boron mass inflow rate is adjusted:

$$\dot{m}_{sticking} = \dot{m} + \dot{m}_{deposition} \tag{18}$$

where $\dot{m}$ is the value obtained from geometric considerations in Eq. 13, and $\dot{m}_{deposition}$ is the total rate of mass deposition on the thruster channel surface. The second term from the right hand side of Eq. 18 is obtained by integrating the incident boron mass flux (computed by MONACO) over the wall surface,

and has a numerical value of 1.71×10^{-10} kg/s. The $\dot{m}_{deposition}$ total value is added to the outer and inner channel wall erosion flow rates in proportions similar to those obtained for the mass flow rate values obtained previously, from geometric considerations.

The erosion inflow number density values for the inner and outer channel walls are obtained for the sticking case, by using Eqs. 14 and 15 with the value of mass flow rate computed from Eq. 18:

$$n_{outer} = 1.45 \times 10^{16} \text{ m}^{-3} \quad (19)$$

$$n_{inner} = 4.83 \times 10^{16} \text{ m}^{-3} \quad (20)$$

Note that the procedure described above to obtain the value of $\dot{m}_{sticking}$ is iterative. The simulation is first run with the initial non-sticking value of $\dot{m}$. This gives the value of deposited boron mass, which is then incorporated in $\dot{m}_{sticking}$ as described in Eq. 18. The computed value of $\dot{m}_{deposition}$ is less than 10% of the value used in the case without sticking, for the first such iteration. Since a second iteration is expected to produce a change of less than 1%, the procedure is not repeated again.

II.B. The MONACO Simulation

An axisymmetric simulation is performed. Two gases are introduced in the MONACO domain: the xenon propellant, and the boron that is eroded from the walls. The time step is set to 3×10^{-7} seconds, and an average number of model particles in the simulation is 1.66×10^6 when boron reflects from the walls, and 6.70×10^5 when the boron neutrals stick. For xenon, the ratio of real to model particles is 10^{10}, whereas for boron the ratio is 1.25×10^6. The simulation is run for 10,000 time steps to reduce the fluctuations in particle numbers during each time step. Then, average values of particle properties are sampled for another 40,000 time steps in order to arrive at the values that are presented in Section III.

II.B.1. Mesh and Boundary Condition Types

A non-uniform triangular mesh is employed, and is shown in Fig. 3. The boundary condition types are labeled on the figure, as follows: SYM for symmetry, IN for inflow, OUT for outflow, WALL for the wall condition and SPUTTER for the eroding wall. The xenon inflow condition introduces particles in the domain with specified number density, temperature and bulk velocity components. The flux used to determine the number of xenon particles introduced is derived from a Maxwellian VDF. The xenon particles are inserted in the domain through an annular section of 0.005 m width, at a rate of 25 sccm, as described in Lee's experimental set-up[2]. In thruster operation, an additional 2 sccm of xenon is introduced through the cathode, and this is neglected in the present study. The outflow condition allows particles to leave the domain. The wall reflects particles, and may also accommodate a certain fraction of the reflected particles to the wall temperature. In the present simulation, all reflected particles are accommodated to the wall temperature which is set to 500 K. The sputter boundary condition combines characteristics of both the inflow and wall boundary types. Particles colliding with the eroding wall are accommodated to the 500 K wall temperature and reflected back into the domain. New boron particles are introduced to the simulation with the particle flux derived from the Sigmund-Thompson distribution, in Eq. 9. For the case where the boron reflects from the walls, the erosion inflow number densities are given in Eqs. 17 and 16, while for the case where the boron neutrals stick to the walls, the inflow number densities are defined in Eqs. 20 and 19. Note that the sticking wall condition is enforced within the simulation by removing all boron particles that reach the wall.

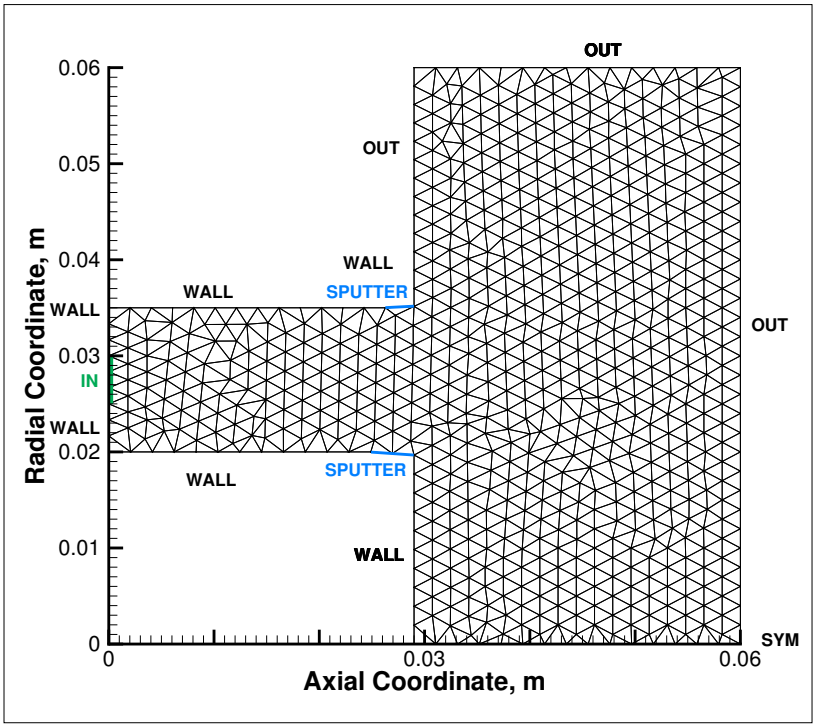

Figure 3: Mesh used in MONACO simulation.

II.C. Path-Integrated Number Density

The CRDS technique yields path-integrated values of the number density (in m^{-2}) in the plume, which may be deconvolved[2] to yield the values of number density (in m^{-3}). Depending on the deconvolution method, numerical errors may be introduced: Lee's[2] results include negative values for the deconvolved number density. Thus for a more realistic comparison, the path-integrated number density values are analyzed instead. Since MONACO outputs number density values, additional processing is required to yield the line integrated values needed for the comparison.

Number density data is extracted from the plume solution along a radial line that starts at the axial coordinate of 0.031 m. This corresponds to the plane in which the CRDS measurements are recorded. Since the simulation is axisymmetric, the data extracted along the line may be copied in a circular pattern to reproduce the azimuthal plane flow-field. Next, the circular flow field is divided into a number of lines that each mimic the CRDS interrogating laser beam. In the present case, 1000 such horizontal lines are defined in between the desired values of the dimensionless geometric parameter P. This variable is defined as:

$$P = \frac{r - r_{in}}{r_{out} - r_{in}} \tag{21}$$

where r is the radial coordinate, r_{in} is the inner channel wall radius and r_{out} is the outer channel wall radius.

Finally, the number density values are integrated numerically along each one of the lines, using trapezoidal integration, to yield the values of path-integrated number density.

III. Results

III.A. Thruster Flow Field

The MONACO simulation output is presented in the form of contour plots of the number density, radial and axial components of the velocity. Moreover, in the velocity plots, streamlines are also shown to illustrate the direction of the flow through the computational domain. The contour plots for xenon flow properties are identical for both cases of boron wall interaction considered (sticking and reflecting from walls). Therefore, only one instance of these results is shown, in Fig. (4). Note that the mean free path for the thruster flow is on the order of 1 m and so there is very little interaction between the xenon and boron atoms. The boron flow field results are compared side by side for the two different wall interaction cases, for each property, and discussed below.

Figure (4a) shows the xenon number density in the simulation domain. The range of values is between 8.0×10^{16} and 1.2×10^{20} m^{-3}. A local maximum may be observed in the region between radial coordinates 0.025 and 0.030 m, and axial coordinates 0 and 0.004 m. This is due to the introduction of xenon particles from the inflow boundary condition, which is defined on the radial axis between the aforementioned coordinates.

Figure (4b) displays a contour plot of the radial velocity values, whose range is between -151 and 254 m/s. It is observed that above the channel centerline, the velocity values are positive, and below they are negative, which is expected because of the expansion of the entering xenon gas particles. The trend is maintained at the thruster exit where another expansion occurs, showing more pronounced differences in the positive and negative values of the radial velocity.

The axial velocity contours for xenon are illustrated in Fig. (4c). The range of values is between -11 and 259 m/s. Note that the thruster centerline serves as an axis of symmetry for the plot. Moreover, since most of the xenon atoms are traveling from left to right in this figure, the axial velocity values are positive, and the streamlines throughout the entire domain are all in the same direction: they start at the xenon inflow boundary and proceed towards the thruster exit.

Figure (5) shows a comparison of the boron number density contours obtained in the two cases considered. In Fig. (5a), where the walls are reflective, the range of values is between 8.3×10^{13} and 1.3×10^{16} m^{-3}. Within the thruster channel, the number density is relatively uniform, with a value larger than 5.0×10^{15} m^{-3}. As the particles exit the thruster, the number density decreases, as expected. In contrast, in Fig. (5b), that results from the sticking case, the range of number density values is between 2.3×10^{13} and 6.0×10^{15} m^{-3}. Here there are two zones of high number density located on the walls, near the thruster exit, where the eroded boron atoms are introduced. Two regions of decreasing density are observed at the two ends of the thruster channel. On the anode side, the decrease occurs because boron particles are leaving the domain through the xenon inflow boundary type or sticking to the walls (which is equivalent to elimination from the domain). On the thruster exit side, the particles are expanding outside the thruster as in the non-sticking case.

Figure (6) presents contours of boron number density, from the azimuthal plane. The data shown is located 2 mm away from the exit plane, at the same location where the CRDS laser interrogates the plume. In Fig. (6a) boron atoms reflect from thruster walls, and the range of number density values is between 1.1×10^{14} and 6.2×10^{15} m^{-3}, while in Fig. (6b), where boron neutrals stick, the range is 3.7×10^{13} to 2.0×10^{15} m^{-3}. A ring of maximum number density is observed in the region corresponding to the channel exit for both cases, but clearly the number density values are much higher in the reflecting wall case, than the sticking simulation. The values then decrease both towards the center of the annular structure, and away from the center, however the absolute minimum is obtained in the outermost ring.

Figure (7) describes the radial velocity values throughout the domain. In Fig. (7a), which corresponds to the reflecting wall case, the range is between -5560 and 2152 m/s. Inside the channel, zones of positive and negative radial velocity alternate. This is because the boron particles being eroded from the inner channel wall, which are more numerous than those from the outer channel wall, move towards the outer wall. Then, the particles are reflected back down, which explains the change in sign for the velocity. In Fig. (7b), which represents the sticking walls case, the velocity range is -7008 to 4921 m/s. Higher velocity values are observed, as well as a different pattern. In the sticking wall case, the radial velocity values become positive on the outer channel wall except for the erosion region, because all the boron particles that travel in that

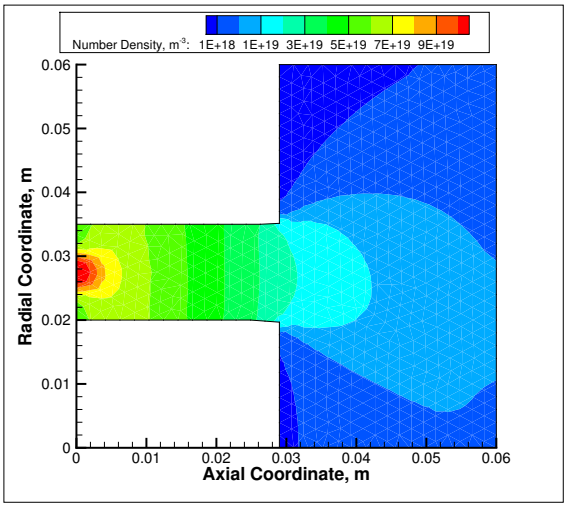

(a) Number density

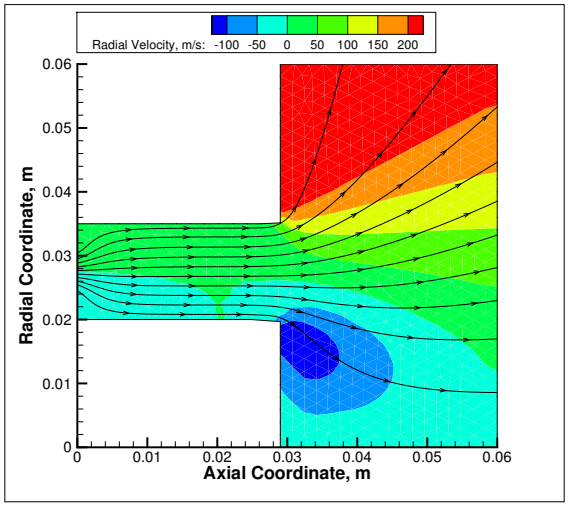

(b) Radial velocity

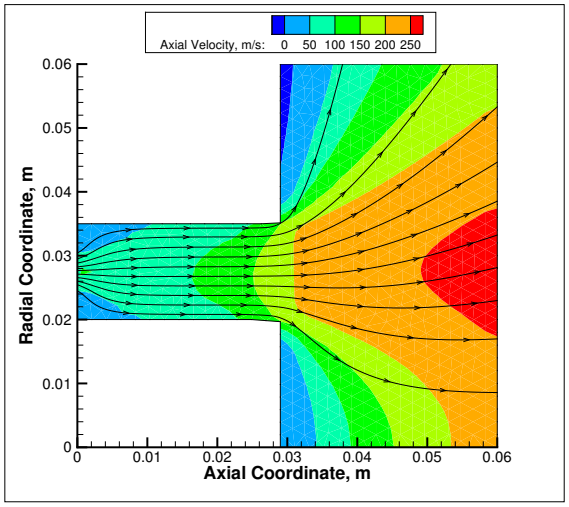

(c) Axial velocity

Figure 4: Xenon flow field contours from MONACO.

direction are removed from the domain upon sticking to the wall. A similar explanation applies for the inner channel wall. In the wall reflection case, these particles return from the wall with a different sign of the radial velocity, which is why the velocity directions alternate more in Fig. (7a).

The boron particle axial velocity contour plots are illustrated in Fig. (8). The range of values in Fig. (8a), where boron atoms do not stick to the walls, is between -505 and 5933 m/s. For axial coordinate values smaller than 0.022 m, the axial velocities are all negative, because the boron atoms are moving towards the anode side, and exiting the domain through the xenon inflow boundary. On the other hand, to the right of the erosion boundary type, the axial velocity has strictly positive values, as the particles traveling through the thruster exit plane move towards the outflow boundaries, to exit the domain. These trends are best illustrated by the streamlines which start on the inner and outer channel walls, where the erosion boundary type is defined, and point either to the left or right sides of the figure, where the boron particles leave the simulation. However, when the boron particles stick to the wall, many streamlines going to the left simply terminate when they reach a wall. This is shown in Fig. (8b), where the range of velocity values is -8017 to $11,136$ m/s. Note also that in the non-sticking cases a recirculation region develops close to the outer channel wall, at the axial coordinate 0.022 m. The boron atoms get trapped due to the wall reflection, in conjunction with the nearby inflow as well as the sputtering from the lower wall. When the boron atoms stick to the wall, this region disappears.

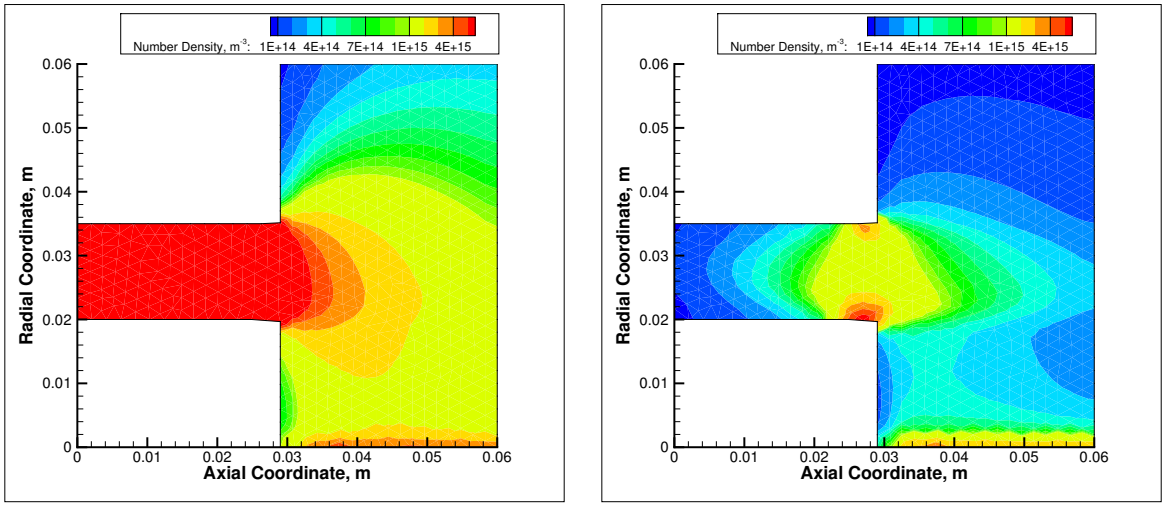

(a) Non-sticking walls. (b) Sticking walls.

Figure 5: Boron number density contours from MONACO.

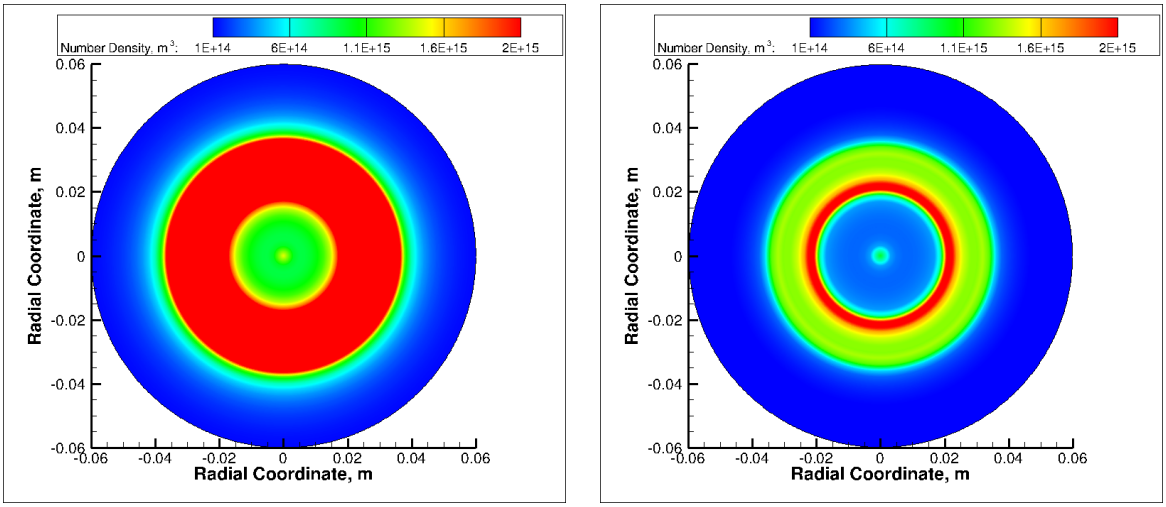

(a) Non-sticking walls. (b) Sticking walls.

Figure 6: Boron number density contours in the azimuthal plane, at an axial coordinate of 0.031 m.

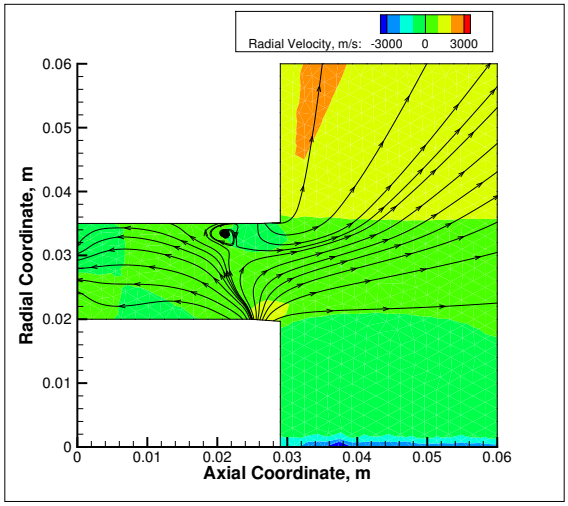

(a) Non-sticking walls.

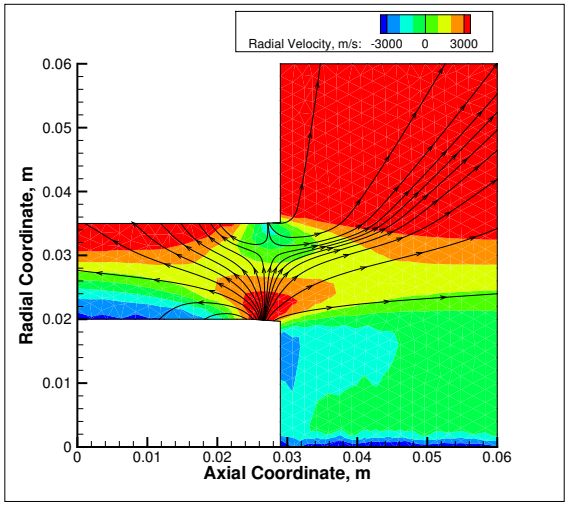

(b) Sticking walls.

Figure 7: Boron radial velocity contours from MONACO.

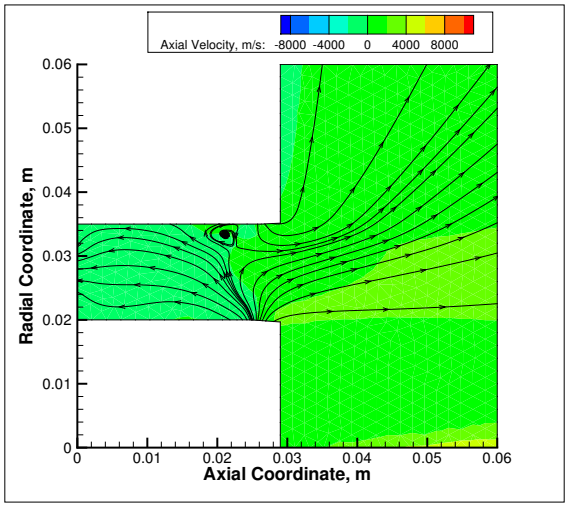

(a) Non-sticking walls.

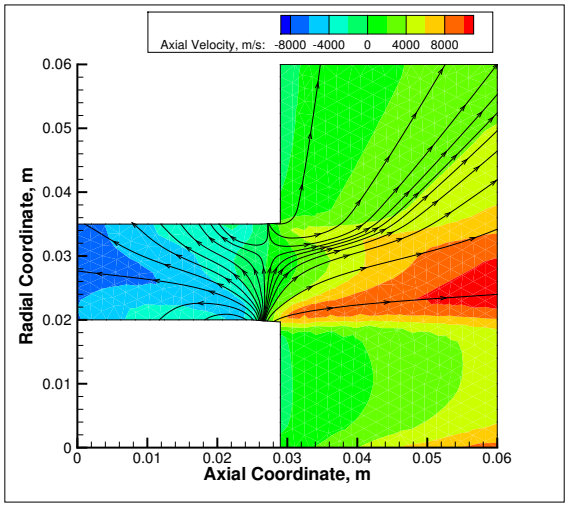

(b) Sticking walls.

Figure 8: Boron axial velocity contours from MONACO.

III.B. CRDS Comparison

The experimental values measured through CRDS are compared in Fig. (9) against the path-integrated values of number density obtained by processing the MONACO data. Good qualitative agreement is observed for both the reflective and sticking walls: both data sets show an increase between $P = -1$ and $P = 0$ that leads to a peak between $P = 0$ and $P = 1$, followed by a steady decrease in the value of line-integrated number density. However, from Fig. (9a) which shows the reflecting wall results, it is clear that the CRDS values are over an order of magnitude lower than those predicted by the MONACO simulation. As seen in Fig. (9b), the simulation results obtained with sticking walls are significantly closer to the measured CRDS values. The number density values differ in magnitude by just a factor of $3 - 4$. There are several plausible sources of the discrepancy. Since the experimental technique is only observing the electronic ground state boron atoms, a number of atoms are excluded from the measurement: those in higher excited electronic states, and those that become ionized. A first order approximate computation of the ionization fraction was performed by using the Saha equation (pp. 162-164 of Ref. [9]). The analysis showed that all of the boron neutrals should ionize. However, since the Saha equation is only applicable to equilibrium mixtures of ions, neutrals and electrons, which is certainly not the case in a SPT-70 HET, it is understood that not all boron atoms will be ionized. Nevertheless, the equilibrium calculation and its results suggest the potential significance that ionization may have. Additionally, uncertainties in some of the simulation input parameters may be affecting the MONACO final results. These factors include the thruster operation time and sputtered boron VDFs, which affect the magnitudes of both the boron particle velocities and flux.

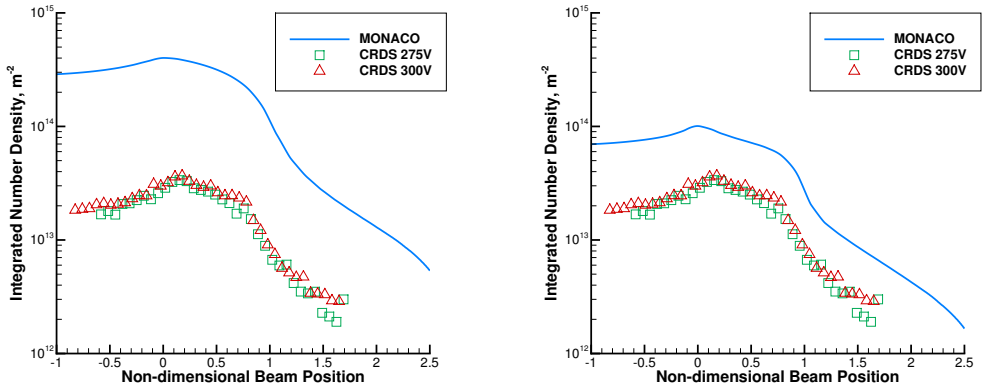

(a) Non-sticking walls.

(b) Sticking walls.

Figure 9: Comparison of integrated values of number density.

IV. Conclusion

The channel erosion of Hall thrusters provides the main lifetime constraint. Identifying the erosion rate may help with mission lifetime predictions, while giving a better understanding of the erosion physics. A new CRDS diagnostic procedure was developed and tested recently[2] for the purpose of measuring path integrated boron number density. The goal is to use such measurements for more efficient and less costly thruster lifetime estimates. However, in order to make lifetime predictions, full knowledge of the flow field is necessary. Hence, a DSMC numerical simulation of the sputtered boron was performed, and the current paper explains the setup and results obtained.

The sputtering process was modeled by using the eroded thruster geometry in the simulation, and introducing the boron particles in a way consistent with the physics of wall sputtering. Hence boron VDFs characteristic to the sputtering process were sampled to assign the velocities of the particles. Moreover, the number flux of boron atoms was computed based on the Sigmund-Thompson distribution which describes the boron velocity component orthogonal to the eroding wall. An estimation of the volumetric erosion rate was carried out based on the current, eroded geometry of the thruster, and the approximate operation time.

Once the simulation produced flow field data for boron and xenon, some processing was required in order

to perform a comparison with the experimental measurements. Data was extracted from the boron number density field in the plane where the CRDS procedure is applied. Then, as an analog to the experimental laser interrogation of the flow field, the data was divided into an arbitrary number of lines (laser beams) over which the number density was integrated.

In the final analysis it was found that the DSMC simulation offers good qualitative agreement with the CRDS technique measurements, however the numerical values differ by an order of magnitude when the boron particles are reflecting from the walls. Another simulation was performed where boron neutrals stick to the walls, upon contact, and the results from this case only differed in magnitude by a factor of $3-4$ from the CRDS data. Several causes for the discrepancy were identified.

There are a number of aspects of the current study that may warrant further work in order to improve the correspondence between simulation and measurement. First, the VDF of the sputtered boron used in the simulation is obtained from a MD simulation conducted at 100 eV energy and 45° angle of incidence. Further MD studies must be conducted to understand the dependence of the sputtered VDFs on the incident ion properties. In addition, the MD simulation must be evaluated against experimental measurements. If the MD simulation predicts higher sputtered boron velocities for the conditions of the SPT-70 thruster, then the line integrated density will decrease and become closer to the CRDS data. Another issue concerns excitation and even ionization processes of ground state boron that are omitted from the simulation. While the mean free paths for these processes are large, on the order of 0.1 to 1 m, there will be a fraction of boron atoms that are excited above the ground state that is not detected by CRDS. Finally, there is considerable uncertainty in the overall mass loss rate of the thruster that is estimated at $\pm 50\%$. The thruster will be operated at a fixed point for several hours in the near future to significantly reduce the uncertainty in this critical parameter. In addition, a full plasma simulation should be prepared in order to account for the electromagnetic interactions that occur in the thruster channel and plume, which have been neglected in the present study.

Acknowledgments

This work was supported by the University of Michigan/AFRL Center of Excellence in Electric Propulsion (MACEEP), through AFRL Grant No. F9550-09-1-0695. H.C.D. thanks Ashley Verhoff for all her patience in answering MONACO related questions, Brandon Smith for providing the sputtered boron VDFs and Dr. Erin Farbar for updating the wall boundary condition to allow sticking.

References

[1]Cho, S., Yokota, S., Hara, K, Takahashi, D., Arakawa, Y., Komurasaki, K., and Kobayashi, A "Hall Thruster Channel Wall Erosion Rate Measurement Method Using Multilayer Coating Chip," *AIAA Joint Propulsion Conference and Exhibit*, AIAA 2010-6697, July 2010.

[2]Lee, B.C., Taylor, J.M., Leach, R.W., Yalin, A.P., and Gallimore, A.D. "Boron Nitride Erosion Measurements of an SPT-70 Hall Thruster via Cavity Ring-Down Spectroscopy," *Joint Army Navy NASA Air Force* (to be published).

[3]Boyd, I. D., Van Gilder, D.B., and Liu, X. "Monte Carlo Simulation of Neutral Xenon Flows in Electric Propulsion Devices," *Journal of Propulsion and Power*, Vol. 14, No. 6, 1998, pp. 1009,1015.

[4]Bird, G. A., *Molecular Gas Dynamics and the Direct Simulation of Gas Flows*, Oxford Univ. Press, Oxford, England, UK, 1994

[5]Yim, J.T., "Computational Modeling of Hall Thruster Channel Wall Erosion," Ph.D. Dissertation, Aerospace Engineering Dept., University of Michigan., Ann Arbor, MI, 2008.

[6]Smith, B. D. and Boyd, I. D., "Computation of Total and Differential Sputter Yields of Boron Nitride Using Molecular Dynamics," *33rd International Electric Propulsion Conference*, IEPC-2013-156, Washington, DC, USA, Oct. 2013.

[7]Tao, L. and Yalin, A., "LIF Velocity Measurement of Sputtered Boron Atoms from Boron Nitride Target," *AIAA Joint Propulsion Conference and Exhibit*, AIAA 2010-6526, July 2010.

[8]Automation Creations, Inc.,"MatWeb, Your Source for Materials Information," *MatWeb Material Property Data* [online database], URL: www.matweb.com [cited 22 August 2013].

[9]Vincenti, W.G. and Kruger, C.H. Jr., *Introduction to Physical Gas Dynamics*, Krieger Publishing Company, Malabar, Florida, 1965